Since January 2020 Elsevier has created a COVID-19 resource centre with free information in English and Mandarin on the novel coronavirus COVID-19. The COVID-19 resource centre is hosted on Elsevier Connect, the company's public news and information website.

Antiviral Research 135 (2016) 108–119

Contents lists available at ScienceDirect

Antiviral Research

journal homepage: www.elsevier.com/locate/antiviral

Intranasal treatment with a novel immunomodulator mediates innate immune protection against lethal pneumonia virus of mice

Elisa C. Martinez [a, b], Ravendra Garg [b], Pratima Shrivastava [b], Susantha Gomis [c], Sylvia van Drunen Littel-van den Hurk [a, b, *]

[a] Department of Microbiology and Immunology, College of Medicine, University of Saskatchewan, Saskatoon, Saskatchewan, 107 Wiggins Road, S7N 5E5, Canada
[b] Vaccine and Infectious Disease Organization-International Vaccine Centre (VIDO-InterVac), University of Saskatchewan, Saskatoon, Saskatchewan, 120 Veterinary Road, S7N 5E3, Canada
[c] Department of Veterinary Pathology, Western College of Veterinary Medicine (WCVM), University of Saskatchewan, Saskatoon, Saskatchewan, 52 Campus Drive, S7N 5B4, Canada

ARTICLE INFO

Article history:
Received 12 July 2016
Received in revised form
7 October 2016
Accepted 18 October 2016
Available online 19 October 2016

Keywords:
PVM
RSV
Immunomodulators
Innate immunity
Protection

ABSTRACT

Respiratory syncytial virus (RSV) is the leading cause of acute lower respiratory tract infections in infants and young children. There are no licensed RSV vaccines available, and the few treatment options for high-risk individuals are either extremely costly or cause severe side effects and toxicity. Immunomodulation mediated by a novel formulation consisting of the toll-like receptor 3 agonist poly(I:C), an innate defense regulator peptide and a polyphosphazene (P-I-P) was evaluated in the context of lethal infection with pneumonia virus of mice (PVM). Intranasal delivery of a single dose of P-I-P protected adult mice against PVM when given 24 h prior to challenge. These animals experienced minimal weight loss, no clinical disease, 100% survival, and reduced lung pathology. Similar clinical outcomes were observed in mice treated up to 3 days prior to infection. P-I-P pre-treatment induced early mRNA and protein expression of key chemokine and cytokine genes, reduced the recruitment of neutrophils and eosinophils, decreased virus titers in the lungs, and modulated the delayed exacerbated nature of PVM disease without any short-term side effects. On day 14 post-infection, P-I-P-treated mice were confirmed to be PVM-free. These results demonstrate the capacity of this formulation to prevent PVM and possibly other viral respiratory infections.

1. Introduction

RSV is the most common cause of bronchiolitis and pneumonia in infants and young children (Garg et al., 2012; Graham and Anderson, 2013). There are no licensed RSV vaccines. The recommended treatment for RSV bronchiolitis is respiratory support and hydration of the patients (Shaw et al., 2013). Palivizumab is used prophylactically exclusively for high-risk infants. Unfortunately, its use is limited to patients in developed countries due to its extremely high cost and logistics of injections (Graham and Anderson, 2013; Shaw et al., 2013; Hurwitz, 2011). Ribavirin is also utilized as a treatment against RSV infections in high-risk young children, but is not very efficient and induces severe adverse effects (Graham and Anderson, 2013; Rosenberg et al., 2005).

Better animal models for the study of RSV pathogenesis can arise from the use of other pneumoviruses matched to their associated hosts, providing a more accurate representation of natural infection and disease (Graham and Anderson, 2013). Pneumonia virus of mice (PVM) has been considered a potential model of RSV infection (Watkiss et al., 2013). PVM is closely related to RSV as both belong to the same viral family and subfamily and induce similar disorders in their natural hosts (Easton et al., 2004; Bem et al., 2011), which makes it a suitable model for the study of RSV-induced inflammation and its contribution to severe respiratory disease outcomes.

We demonstrated that a novel adjuvant platform in combination with the RSV fusion protein induces long-lasting immune responses against RSV in several animal models (Garg et al., 2014a,

* Corresponding author. VIDO-InterVac, University of Saskatchewan, 120 Veterinary Road, Saskatoon, S7N 5E3, Canada.
E-mail address: sylvia.vandenhurk@usask.ca (S. van Drunen Littel-van den Hurk).

http://dx.doi.org/10.1016/j.antiviral.2016.10.008
0166-3542/

2014b, 2015). The first component of this formulation is poly(I:C), which promotes Th1 immune responses by inducing high levels of IL-12 and type I IFNs (Zhao et al., 2012; Tewari et al., 2010). The second component is an innate defense regulator (IDR) peptide, which is a derivative of bovine bactenecin and possesses immunomodulatory properties (Nijnik et al., 2010; Wu and Hancock, 1999; Hilchie et al., 2013). Lastly, this adjuvant platform contains poly[di(sodiumcarboxylatoethylphenoxy)]-phosphazene (PCEP), a synthetic water-soluble polymer that acts as a delivery system and can modulate innate immune responses (Mutwiri et al., 2007; Awate et al., 2012). The combination of poly(I:C), IDR peptide and PCEP (P-I-P) generates an immunomodulator with potential as an alternative strategy to prevent infectious diseases.

In the current study we assessed the potential of P-I-P to protect Balb/c mice against a lethal PVM-15 infection based on clinical disease and viral replication. We also examined the nature of the inflammatory response induced by P-I-P treatment to delineate a possible mechanism of action of this formulation.

2. Materials and methods

2.1. Cell line and virus

PVM-15 was propagated in Baby Hamster Kidney 21 (BHK-21, ATCC, Manassas, VA, USA) cells in Dulbecco's Modified Eagle Medium (DMEM, Sigma-Aldrich, St. Louis, MO, USA) containing 2% fetal bovine serum, 0.1 mM non-essential amino acids, 10 mM HEPES, and 50 μg/mL gentamicin (Thermo Fisher Scientific, Waltham, MA, USA) (Watkiss et al., 2013; Shrivastava et al., 2015).

2.2. Treatment formulations and PVM-15 challenge

Five to six week-old female Balb/c mice (Charles River Laboratories, Saint-Constant, QC, Canada) were given 20 μl of phosphate-buffered saline (PBS, Thermo Fisher Scientific) or P-I-P intranasally, and lungs were collected at selected time points. To evaluate the ability of P-I-P to elicit protection from viral infection, mice were given intranasal treatments of PBS or P-I-P, and challenged 1, 3, 4, 5, or 6 days later with 3000 pfu of PVM-15 in 50 μl. The P-I-P formulation contained 20 μg poly(I:C) (Invivogen, San Diego, CA, USA), 40 μg IDR peptide 1002 (Genscript, Piscataway, NJ, USA), and 20 μg PCEP (Idaho National Laboratory, Idaho Falls, ID, USA) in PBS. The 1:2:1 ratio of the P-I-P formulation is optimal when used as an adjuvant (Kovacs-Nolan et al., 2009). A full description of treatment groups in the experiments is provided in Table S1.

Five mice per group were scored and weighed daily according to a modified version of *Morton and Griffith's* guidelines (Morton and Griffiths, 1985). On day 14 post-infection (p.i.), all remaining mice were euthanized, and in some cases, the lungs of surviving mice were collected for further analysis. All animal trials were conducted in accordance with the Canadian Council on Animal Care.

2.3. Collection and processing of lung samples

At 6, 24, 96 and 144 h post-treatment (p.t.) or on days 0, 3 and 5 p.i. the single-lobed lung was collected into TRIzol® reagent (Thermo Fisher Scientific) for gene expression studies and the multi-lobed lung was collected for virus titrations and multiplex ELISAs. Both lungs were homogenized using a mini bead-beater (BioSpec Products Inc., Bartlesville, OK, USA), and centrifuged at 4 °C to remove gross debris. Immediately, all samples were aliquoted, flash-frozen in liquid nitrogen and stored at -80 °C.

2.4. Viral titrations and PVM qPCR assays

PVM titrations were performed as described previously (Watkiss et al., 2013; Shrivastava et al., 2015). Absolute PVM copy numbers were calculated via quantitative real-time PCR (qPCR) using a 1:5 serial dilution standard curve of stock PVM RNA in nanograms. The primers were specific to the small hydrophobic (SH) gene of the virus. Unknown RNA concentrations were calculated following the equation of the curve, and copy numbers were determined according to Avogadro's number and the SH gene amplicon size.

	P-I-P				PBS			
	6 hr p.t.	24 hr p.t.	96 hr p.t.	144 hr p.t.	6 hr p.t.	24 hr p.t.	96 hr p.t.	144 hr p.t.
CCL2	67.65	94.88	19.92	24.59	0.97	1.16	0.93	0.99
CCL3	7.7	15.22	6.18	4.02	1.86	0.91	1.13	1.29
CXCL2	10.7	14.56	2.12	4.14	2.3	1.14	0.96	1.06
CXCL1	23.39	32.67	4.2	6.31	0.93	1.17	0.9	1.04
CXCL10	1765.67	329.01	29.12	19.11	2.12	1.02	1.23	1.18
TNF-α	11.88	7.7	3.83	6.69	1.59	1.14	0.97	0.99
IL-1β	16.73	13.18	1.84	2.03	0.56	0.97	1.02	1.3
IL-6	50.49	44.02	7.02	7.34	0.88	0.97	1.37	0.99
IL-12β (p40)	14.58	13.91	14.34	7.7	2.02	1.04	1.06	0.88
IL-10	9.22	7.78	4.28	33.78	1.60	1.23	1.04	1.18
TGF-β	0.97	1.77	0.76	0.58	1.14	0.86	1.29	1.22
IFN-α	9.62	51.13	1.55	0.69	1.07	1.32	0.94	1.28
IFN-β	278.59	195.09	11.2	4.46	1.02	1.23	1.07	0.85
IFN-γ	58.65	6.32	2.73	9.32	1.08	1.07	1.11	0.99

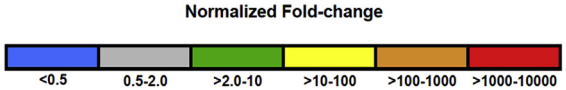

Fig. 1. Heat map of chemokine and cytokine mRNA expression profiles in the single-lobed lungs of 5–6 week-old female Balb/c mice at 6, 24, 96 and 144 h p.t. with either P-I-P or PBS. Each treatment group contained 20 mice in total, with sampling of 5 animals at each time-point indicated above. All Ct values were normalized against β-actin levels of control animals. Normalized fold-change calculations were performed using the $2^{-\Delta\Delta Ct}$ method. Data are shown as the median of five biological replicates.

2.5. Chemokine, cytokine and interferon qPCR

Total RNA was extracted from the single-lobed lung in TRIzol® reagent (Thermo Fisher Scientific). Complementary DNA (cDNA) synthesis was performed using the QuantiTect Reverse Transcription kit (Qiagen, Venlo, Limburg, Netherlands). qPCR was carried out using FastStart SYBR Green Master (Roche, Basel, Switzerland). The primers (Thermo Fisher Scientific) and annealing temperatures used in the experiments are listed in Table S2. All results were normalized against the average β-actin levels of the PBS or PBS/Medium control animals.

2.6. Multiplex ELISAs

Multi-lobed lungs were homogenized in DMEM, aliquoted with 1× SIGMA*FAST*™ Protease Inhibitor solution (Sigma-Aldrich) and flash-frozen on days 0, 3 and 5 p.i. The MSD Multi-Spot V-PLEX assay for the pro-inflammatory panel 1 (TNF-α, IL-1β, IL-6, IL-12, IL-

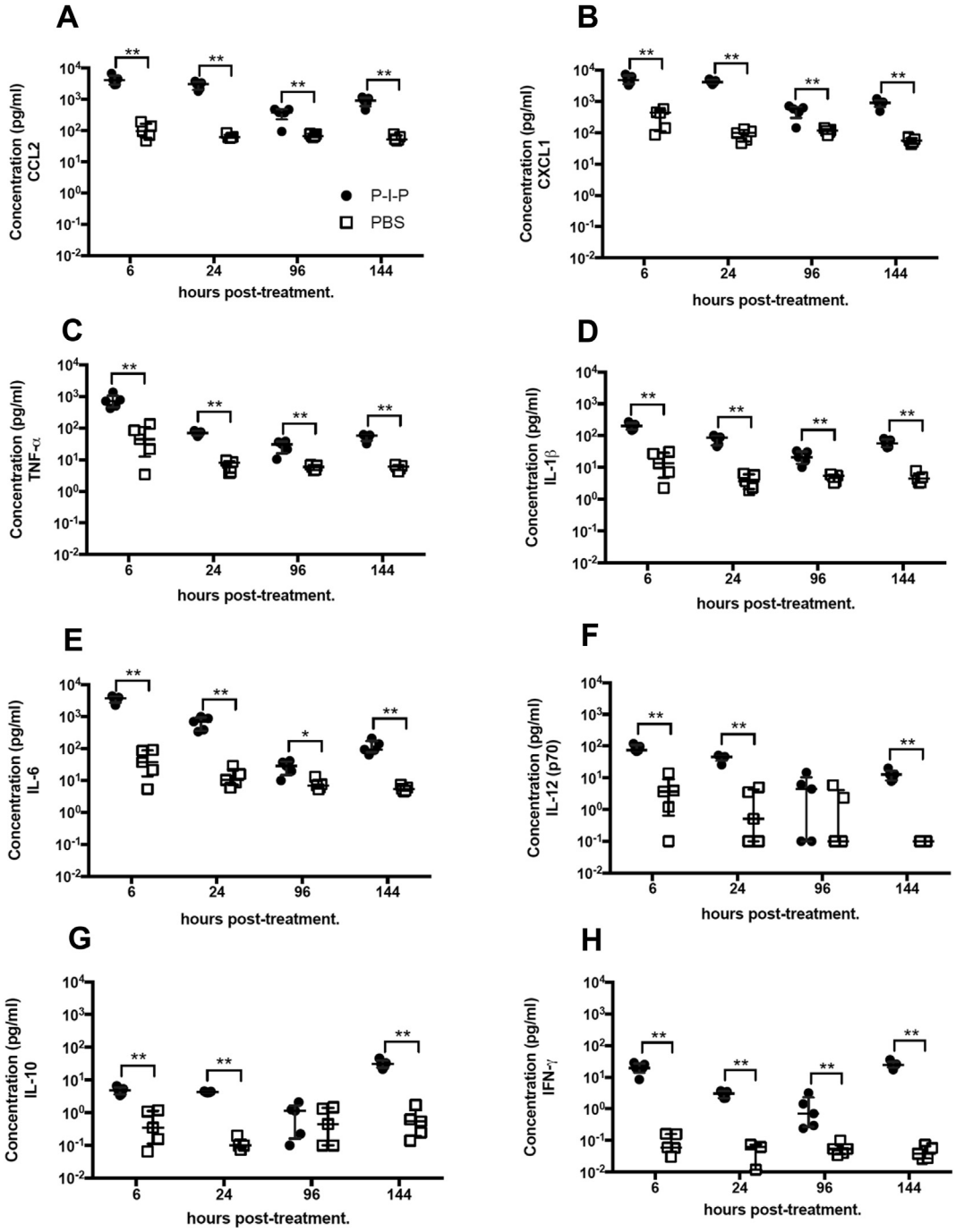

Fig. 2. Protein expression levels of chemokine and cytokine genes in lung homogenates at 6, 24, 96 and 144 h p.t. Mice were given intranasal treatment of PBS or P-I-P and the multi-lobed lungs of 5 mice per group were collected separately for each individual animal at the time points indicated. Protein expression was assayed by electrochemiluminescence-based multiplex ELISAs. Panels A to H represent protein expression data in pg/mL for CCL2, CXCL1, TNF-α, IL-1β, IL-6, total IL-12 (p70), IL-10, and IFN-γ, respectively. Data are shown as individual values representing single animals as well as median with interquartile range of five biological replicates. $^{*}p < 0.05$, $^{**}p < 0.01$.

10 and CXCL1) and the MSD Multi-Array Mouse Cytokine Ultra-sensitive Assay for CCL2 were used to quantify cytokine, type II IFN, and chemokine levels in the lungs (Meso Scale Discovery, Rockville, MD, USA).

2.7. Processing of lungs and flow cytometry

Lung single-cell suspensions were generated as previously described (Watkiss et al., 2013; Shrivastava et al., 2015). To identify different leukocyte populations, the cells were blocked with TrueStain fcX (Biolegend, San Diego, CA, USA) and stained with their corresponding fluorochrome-conjugated antibody cocktails (Table S3). Flow cytometry was performed using a FACS Calibur (BD Biosciences, Franklin Lakes, NJ, USA). Analysis of flow cytometry data was performed using Kaluza software (Beckman Coulter Inc., Pasadena, CA, USA).

2.8. Histology

The multi-lobed lung was perfused with 10% neutral buffered formalin (NBF, VWR, Radnor, PA, USA) and collected on day 1 p.t. or day 6 p.i. The perfused lungs were embedded in paraffin, sectioned into duplicate 5 μm sections, stained with hematoxylin and eosin (H&E), and scored in a blinded manner by a veterinary pathologist. Scores were given based on the presence, severity, and distribution of lesions in each lung lobe. A score of 0 denotes a normal lung. Scores 1 through 3 represent signs of mild, moderate, and severe perivascular edema, perivasculitis, and cellular infiltration within the pulmonary parenchyma, respectively.

2.9. Statistical analysis

GraphPad Prism 6 was used to analyze all the data (GraphPad Software, Inc., La Jolla, CA, USA). Differences among groups were assessed using Student t-tests, one-way ANOVAs and the Newman-Keuls method for multiple comparisons. Differences were considered significant at $P < 0.05$.

3. Results

3.1. P-I-P promotes the expression of pro-inflammatory cytokines and chemokines in the lung milieu

Mice were treated intranasally with P-I-P, and at 6, 24, 96 and 144 h p.t., gene and protein expression profiles of selected cytokines and chemokines were monitored. For CXCL10, highest gene expression was detected 6 h p.t, while highest mRNA production for CCL2, CCL3, CXCL1 and CXCL2 was detected at 24 h p.t. (Fig. 1).

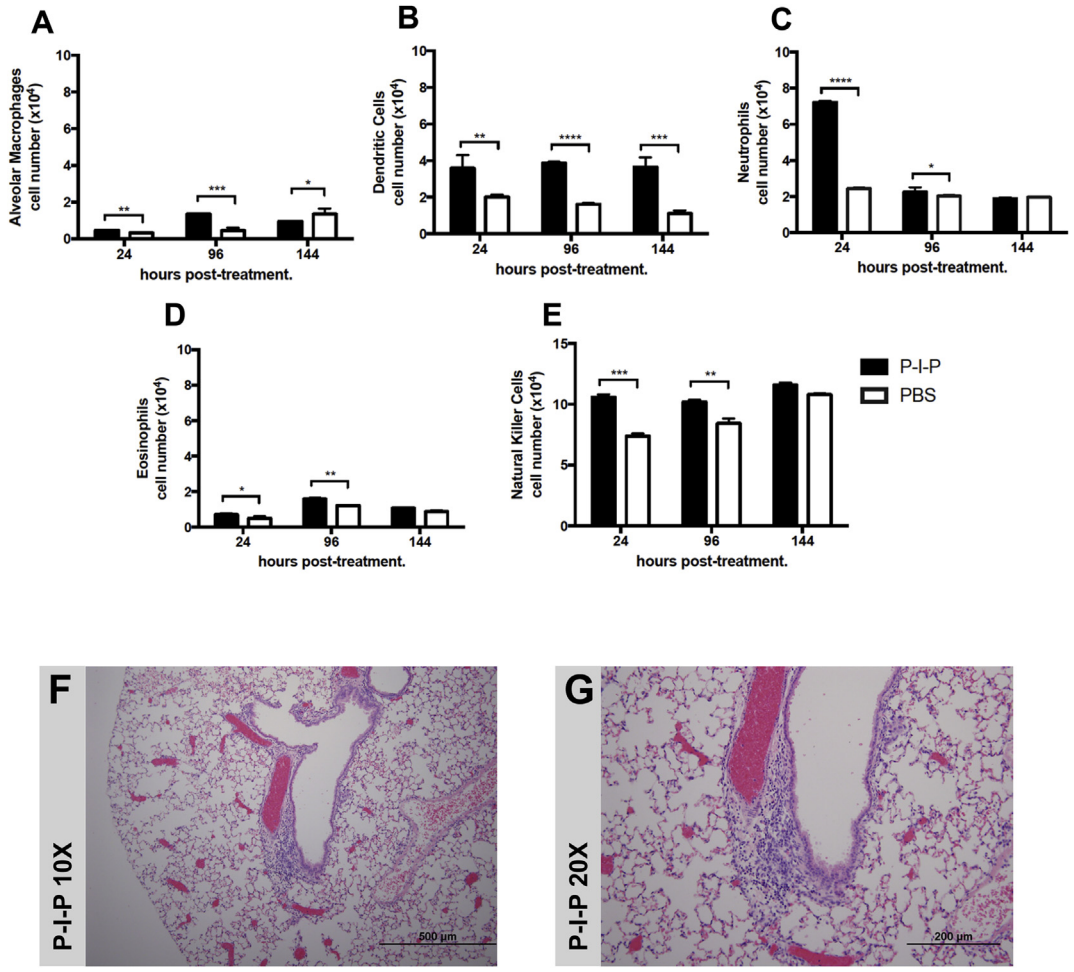

Fig. 3. Effects of P-I-P treatment on cellular recruitment of immune cells and histology of the lung tissue. Mice were given an intranasal treatment of PBS or P-I-P and the lungs of 3 mice per group were collected, pooled, and processed at the time points indicated. Total numbers of alveolar macrophages (A), DCs (B), neutrophils (C), eosinophils (D), and NK cells (E) in the lungs were analyzed by flow cytometry. Results are presented as cell number x 10^4 per million cells. For histology experiments, five mice per group were treated as previously described and at 24 h p.t., the multi-lobed lung was collected. Panels F & G represent lung histology sections at 10× and 20× magnifications, respectively, for the P-I-P group. Data are shown as the median with interquartile range of three technical replicates per cell type assayed. *$p < 0.05$, **$p < 0.01$, ***$p < 0.001$, ****$p < 0.0001$.

Similarly, highest protein expression for CCL2 and CXCL1 was detected within the first 24 h following P-I-P treatment (Fig. 2A, B). However, by the 96-hr time point, CCL2 and CXCL1 protein concentrations decreased by 86% and 88%, respectively.

Furthermore, P-I-P treatment induced moderate upregulation of TNF-α, IL-1β, IL-6 and IL-12β mRNA at 6 and 24 h p.t. These levels decreased at later time points (Fig. 1). Highest protein concentrations for TNF-α, IL-1β, and IL-6 were detected at 6 h p.t. (Fig. 2C–E), and by 24 h, these amounts significantly decreased, by 90%, 57% and 82%, respectively. At 96 h p.t., the levels of these cytokines further decreased. The IL-12p70 protein concentration was 75 pg/ml at 6 h p.t. During the next two time points, its quantity was significantly reduced by 38% and 90%, respectively (Fig. 2F).

Interestingly, IL-10 mRNA was moderately upregulated within the first 96 h p.t., and increased to approximately 34-fold at 144 h p.t. (Fig. 1). Similarly, IL-10 protein concentrations were highest at the 144-hr time-point (Fig. 2G). The delayed expression of IL-10 can be attributed to its unique role in dampening immune responses *in vivo*.

The highest level of IFN-α mRNA expression was detected at 24 h p.t., but maximal IFN-β mRNA expression occurred at 6 h p.t. IFN-γ mRNA also reached its peak at 6 h p.t and by 24 h p.t., mRNA levels strongly declined (Fig. 1). Similarly, IFN-γ protein production was highest at 6 h p.t., followed by a significant continuous decrease thereafter (Fig. 2H).

3.2. P-I-P mediates immune cell infiltration into the lungs of mice without causing toxicity

The number of alveolar macrophages, dendritic cells (DCs), neutrophils, eosinophils and natural killer (NK) cells in the tissue were quantified. Alveolar macrophage and eosinophil numbers were low and peaked at 96 h p.t. (Fig. 3A,D), while DC and NK cell counts were increased at 24 h p.t. and remained steady during the 6 days following P-I-P treatment (Fig. 3B,E). Neutrophil numbers peaked at 24 h p.t. and declined significantly overtime (Fig. 3C).

Considering that the neutrophil number in the lung was higher at 24 h p.t., a histology study was performed to determine if this event lead to lesions or toxicity *in vivo*. At 24 h p.t., a mild form of lymphocytic perivasculitis and peribronchiolitis was observed (Fig. 3F,G). These lesions were not life-threatening and are suggestive of increased cellular recruitment. It can be concluded that P-

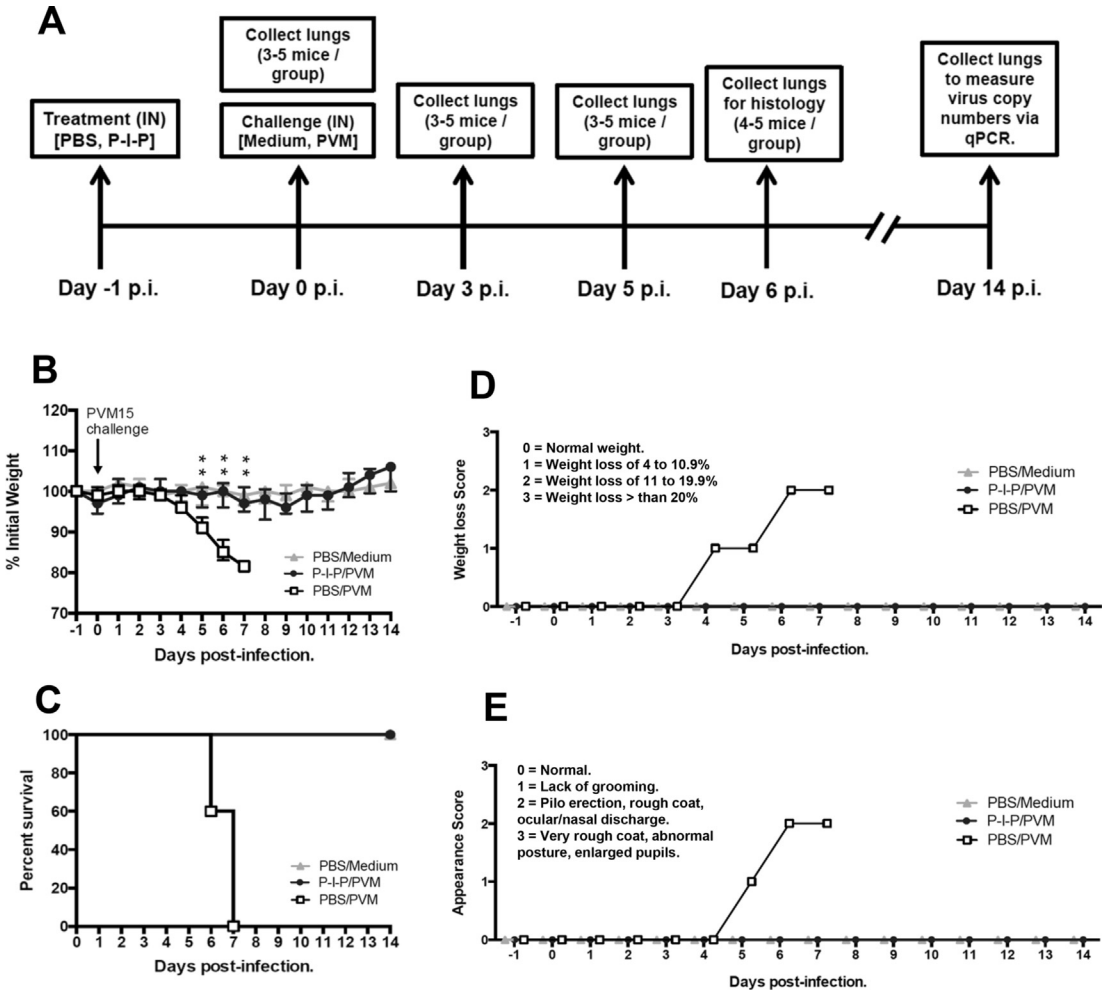

Fig. 4. Outline of trial, weight change, clinical and survival scores of P-I-P- or PBS-treated Balb/c mice before and after intranasal PVM challenge. Mice were given intranasal treatment of P-I-P or PBS 24 h prior to challenge with 3000 pfu PVM-15. Animals were weighed and scored before treatment (i.e. day -1), on the day of challenge (i.e. day 0), and for 14 days after infection. Panel A highlights the events occurring in the animal trial. Collection of lung tissue for virus titrations, cell influx and mRNA/protein expression studies was scheduled on days 0 (prior to infection), 3 and 5 p.i. Lung samples for histopathology studies were collected on day 6 p.i. On day 14 p.i., qPCR was performed on survivor mice to determine their PVM status. Panel B illustrates weight loss of mice following P-I-P treatment and PVM infection as a median percentage of the starting weight with error bars indicating the interquartile range. The stars indicate the difference between P-I-P/PVM and PBS/PVM groups. Panel C represents survival rates as the median percentage of the total number of animals per group during the 14 days following infection. Panels D and E show clinical scores for weight loss and appearance represented by the median value for each group throughout the entire animal trial. Each experiment was performed twice, with an average of n = 5, and a total number of animals equal to 10 per group. $^{**}p < 0.01$.

I-P induces a controlled inflammatory response that has no impact on the appearance, behaviour or body weight of the animals.

3.3. P-I-P protects adult Balb/c mice against a lethal PVM infection

Subsequently, we examined whether P-I-P pre-treatment might protect Balb/c mice from lethal PVM challenge. We delivered the treatment 24 h prior to virus inoculation as chemokine and cytokine mRNA and protein levels were high yet displaying a more balanced profile than that detected at 6 h p.t. P-I-P-treated animals exhibited minimal weight loss (Fig. 4B), no overt signs of clinical disease (Fig. 4D,E), and 100% survival by day 14 p.i. (Fig. 4C). The P-I-P-treated mice had significantly lower numbers of viable virions and viral mRNA copies in their lungs when compared to the PBS-treated group (Fig. 5A,B). On day 14 p.i., lung homogenates of survivor mice were PCR-negative for PVM-15 mRNA, suggesting that P-I-P pre-treatment promotes complete clearance of the virus *in vivo* (data not shown).

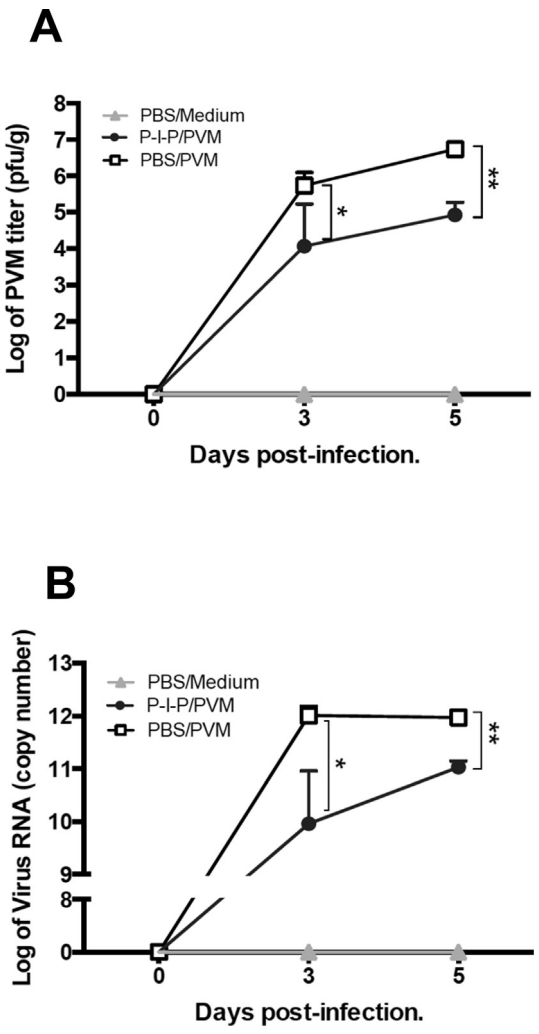

Fig. 5. PVM titers and absolute virus copy numbers in the lungs of P-I-P pre-treated Balb/c mice on days 0 (prior to infection), 3 and 5 p.i. The multi-lobed lung was homogenized in DMEM and used for virus titrations. Panel A shows the log of PVM titers in the lung tissue expressed in pfu/g. The single-lobed lung was processed in TRIzol and used for qPCR. Panel B shows the log of absolute PVM mRNA copy numbers, which were determined as described in the Materials and Methods section. Data are represented as the median with interquartile range of five biological replicates per group. Each experiment was repeated twice. $^{*}p < 0.05$, $^{**}p < 0.01$.

3.4. P-I-P reduces the severity and magnitude of lung lesions in the lungs of Balb/c mice lethally infected with PVM

The lung pathology induced by PVM infection in P-I-P- and PBS-treated mice was examined in a subsequent trial. The lungs of the P-I-P/PVM group showed peribronchiolitis and perivasculitis; lymphocytic, multifocal, subacute to chronic. This indicates a mild reaction and chronicity with no indication of functional problems (Fig. 6C,D). In contrast, the PBS/PVM group had signs of perivascular edema, perivasculitis, and limited cellular infiltration within the pulmonary parenchyma. This is an acute severe reaction indicating pulmonary damage and functional problems (Fig. 6E–G). It can be noted that a large portion of the infiltrating cells are polymorphonuclear leukocytes (PMNs), mostly in the form of neutrophil granulocytes (Fig. 6F,G). There was a statistically significant difference in lung pathology between P-I-P-treated and PBS-treated PVM-infected mice, suggesting that treatment with P-I-P reduces the number and severity of lesions in the lungs following an otherwise lethal PVM infection (Fig. 6H).

3.5. P-I-P pre-treatment promotes early upregulation of chemokines, pro-inflammatory cytokines, and interferons, modulating the immune responses to PVM

The nature of the immune responses induced by P-I-P after a lethal PVM infection was also examined at the gene and protein level. P-I-P-treated mice showed early upregulation of CCL2, CCL3, CXCL1, CXCL2 and CXCL10 mRNA on day 0 p.i., compared to the PBS-treated animals. This was confirmed for CCL2 and CXCL1 at the protein level. During the next two time points following PVM infection, chemokine expression remained fairly stable and did not change over time (Figs. 7 and 8A,B). In contrast, PBS-treated mice expressed increasing amounts of these two chemokine molecules over time (Figs. 7 and 8A,B).

P-I-P-treated animals displayed slightly upregulated mRNA levels for TNF-α, IL-1β, IL-6, IL-12 and IL-10 on day 0 p.i. (Fig. 7). Similarly, higher cytokine protein concentrations were detected in these mice on day 0 p.i. compared to PBS-treated mice (Fig. 8C–G). With the exception of IL-10, which increased over time, the P-I-P-treated group continued to have relatively stable cytokine gene and protein expression profiles throughout the remaining days following PVM infection. Conversely, cytokine gene and protein expression profiles of the PBS-treated group were characterized by increasing levels of these molecules over time, with highest overall expression detected on day 5 p.i. Overall, P-I-P-treated mice displayed lower cytokine protein concentrations on day 5 p.i. compared to the PBS-treated animals.

P-I-P-treated animals displayed an earlier expression of type I IFN mRNA compared to PBS-treated mice (Fig. 7). By day 3 p.i., these mice experienced a significant drop in both IFN-α and IFN-β mRNA levels. In contrast, the PBS-treated animals showed a slightly delayed expression of type I IFNs, with highest IFN-α and IFN-β mRNA expression on days 3 and 5 p.i., respectively. P-I-P-treated mice displayed elevated levels of both IFN-γ mRNA and protein on day 0 p.i., significantly higher than those detected in PBS-treated animals (Figs. 7 and 8H). In contrast, in the PBS-treated mice IFN-γ mRNA and protein expression was highest on day 5 p.i.

3.6. P-I-P reduces the influx of neutrophils and eosinophils into the lungs of Balb/c mice during a lethal PVM infection

In view of the significant infiltration of PMNs into the lungs of PBS-treated PVM-infected mice, the influx of different innate immune cells into the lungs was measured. P-I-P-treated mice showed increased numbers of alveolar macrophages on day 0 p.i., which

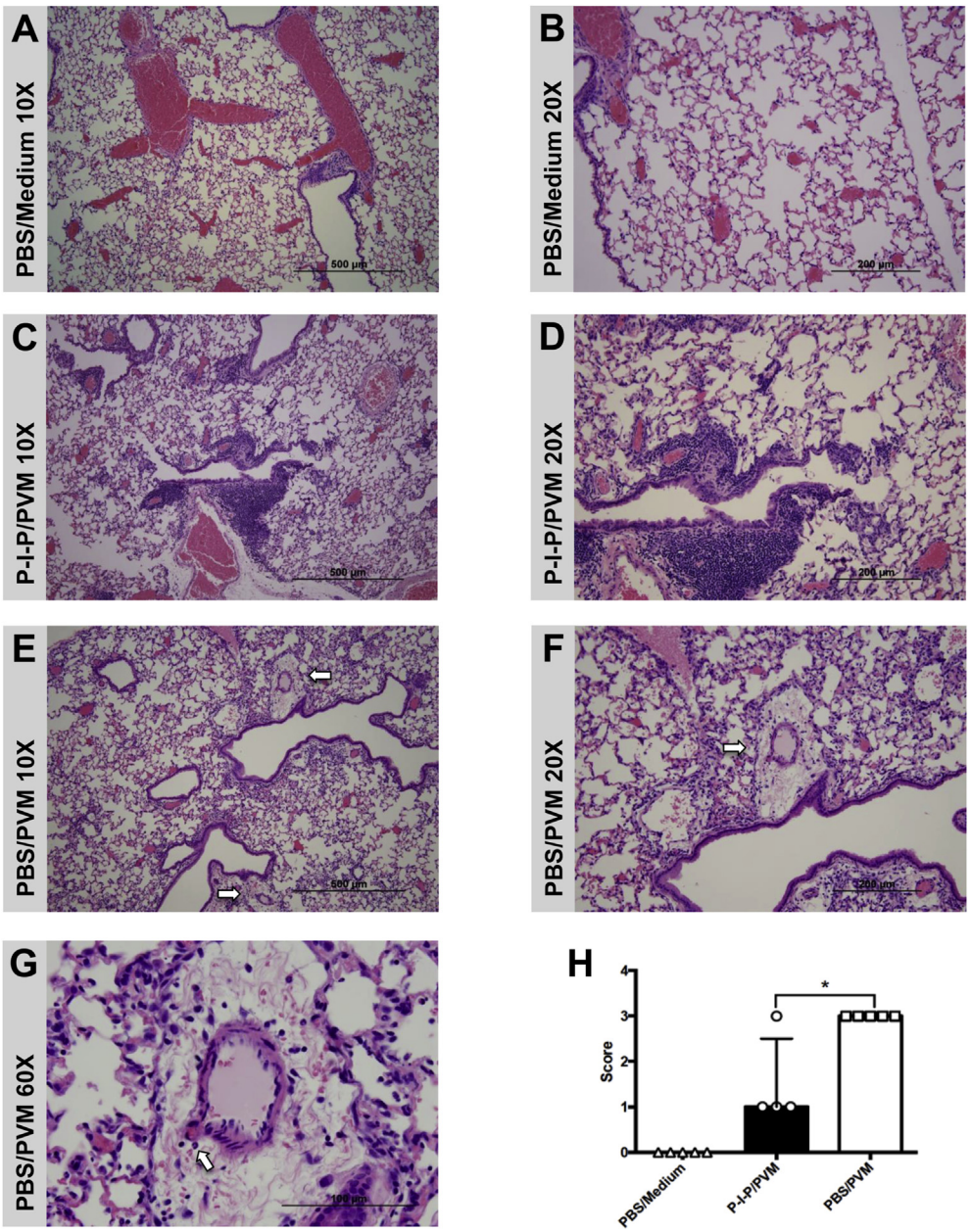

Fig. 6. Lung pathology of Balb/c mice pre-treated with P-I-P or PBS 24 h prior to intranasal PVM challenge. Four to five mice per group were treated as previously described and infected intranasally with 3000 pfu of PVM. All lung samples were collected on day 6 p.i. Panels A & B represent lung sections at 10× and 20× magnifications, respectively, for the PBS/Medium control group. Panels C & D show lung sections at 10× and 20× magnifications, respectively of mice treated with P-I-P. Panels E to G illustrate lung sections of PBS-treated mice at 10×, 20× and 60× magnifications, respectively. White arrows point to several areas of edema in the tissue, as well as PMNs within this region. Panel H shows the lung histopathology scores given on the basis of the severity and dissemination of the lesions visible in duplicate lung sections. Data are represented as both individual and median values for each group with error bars indicating the interquartile range. $^{*}p < 0.05$.

peaked on day 3 p.i. (Fig. 9A). Furthermore, P-I-P treatment mediated early DC influx into the lungs of these mice, with numbers significantly higher than the PBS-treated PVM-infected animals (Fig. 9B). In P-I-P-treated animals, neutrophil infiltration was characterized by an early transient recruitment into the lungs prior to PVM infection, and after PVM challenge these numbers tended to decrease and level off. In contrast, PBS-treated PVM-infected mice started with low neutrophil counts, and as the infection progressed, these values drastically increased over time (Fig. 9C). On day 5 p.i., PBS-treated PVM-infected mice had greatly elevated levels of neutrophils in the lungs, suggesting neutrophilia. Eosinophil numbers of PBS-treated PVM-infected mice went up on day 3 p.i., and continued to increase thereafter. However, P-I-P-treated animals displayed very little eosinophil recruitment, similar to that of the PBS/Medium group (Fig. 9D). Lastly, P-I-P treatment induced recruitment of NK cells into the lungs on day 0 p.i. By days 3 and 5 p.i., NK cell influx decreased, reaching numbers comparable to those in the PBS/Medium group. Interestingly, PBS-treated PVM-challenged mice had delayed NK cell recruitment, with highest numbers on day 5 p.i. (Fig. 9E).

3.7. Weight loss and mortality increase when P-I-P treatment is delivered at earlier time points prior to PVM infection

We further investigated the duration of protection that P-I-P is capable of conferring to mice lethally infected with PVM. Animals

A	P-I-P/PVM			PBS/PVM		
	Day 0 p.i.	Day 3 p.i.	Day 5 p.i.	Day 0 p.i.	Day 3 p.i.	Day 5 p.i.
CCL2	39.60	15.43	30.70	1.49	28.21	471.14
CCL3	4.67	6.99	9.69	1.37	5.34	25.56
CXCL2	4.45	7.7	6.22	1.56	24.83	145.61
CXCL1	15.30	10.85	11.36	1.01	29.04	70.82
CXCL10	100.08	22.63	73.93	0.87	64.45	1661.19
TNF-α	7.5	5.7	8.36	0.75	5.99	19.35
IL-1β	4.09	1.77	3.51	1.36	1.49	7.47
IL-6	12.36	6.35	9.18	1.57	21.50	316.93
IL-12β (p40)	6.66	4.9	8.41	0.86	2.22	13.20
IL-10	3.57	4.78	36.25	0.86	4.78	50.56
TGF-β	0.69	0.9	0.83	0.97	0.91	0.89
IFN-α	19.19	1.13	2.6	1.08	23.59	7.72
IFN-β	109.14	6.22	10.50	1.16	21.08	91.90
IFN-γ	3.9	5.51	10.48	0.97	4.73	24.59

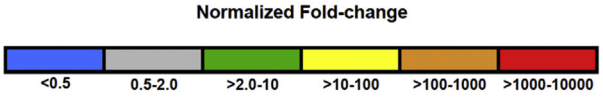

Fig. 7. Heat map of chemokine and cytokine mRNA expression profiles of P-I-P- or PBS-treated Balb/c mice before and after intranasal PVM challenge. Mice were given an intranasal treatment of PBS or P-I-P 24 h before challenge with 3000 pfu PVM. The single-lobed lungs of 5 mice per group were collected on days 0 (prior to infection), 3 and 5 p.i. All Ct values were normalized against β-actin levels of control animals. Normalized fold-change calculations were performed using the $2^{-\Delta\Delta Ct}$ method. Data are shown as the median of five biological replicates.

treated 3 days prior to infection experienced less than 10% weight loss and 90% survival (Fig. 10A,B). These mice had low clinical scores for appearance (Fig. 10C). Mice treated 4, 5 or 6 days prior to challenge had a further gradual increase in weight loss and clinical scores, and lower survival rates (Fig. 10D–L). Regardless of the day of the treatment, survivor mice of the day -3 and -6 trials were PVM-negative on day 14 p.i. These experiment show that P-I-P still has good activity up to 3 days prior to infection.

4. Discussion

In the present study we assessed the potential of a novel immunomodulatory compound, P-I-P, in a PVM disease model as an alternative approach to prevent severe respiratory infections. P-I-P significantly upregulated the expression of genes involved in host defense within the first 24 h p.t. Thereafter, these levels decreased as expected due to their relatively short half-lives. P-I-P prophylaxis at 24 h prior to PVM challenge prevented weight loss and clinical symptoms, reduced lung immunopathology, and conferred complete survival. Additionally, P-I-P was found to be a superior formulation compared to poly(I:C), IDR peptide or PCEP alone (data not shown). P-I-P did not cause any observable adverse effects as evidenced by the absence of clinical signs following treatment. Interestingly, P-I-P mediated a substantial reduction of neutrophil and eosinophil influx during PVM infection, and induced the early recruitment of NK cells and DCs into the lungs. Lastly, the protective effect of P-I-P was maintained if delivered as early as 3 days prior to lethal challenge. Survivor mice were deemed PVM-free on day 14 p.i. This suggests that P-I-P modulation of host immune responses can trigger complete clearance of the virus from the site of infection.

Most immunomodulatory regimes have two major goals: enhance pathogen clearance and suppress undesirable immune responses. With regards to PVM as well as RSV, an effective therapeutic approach should be both antiviral and immunomodulatory in nature (Rosenberg et al., 2005; Bonville et al., 2003). One group demonstrated this principle for PVM by injecting mice with ribavirin together with CCL3 blockade by either gene-deletion or antibody (Bonville et al., 2003). In order to achieve the desired outcomes, two daily doses of ribavirin and a single daily dose of anti-CCL3 antibody were required during a period of 12 days (Bonville et al., 2003). As mentioned previously, ribavirin is known to induce toxicity and severe side effects in pediatric patients, discouraging its use in these populations. A few advantages of P-I-P treatment include the fact that it indirectly induces moderate antiviral activity and can down-modulate the levels of chemokines and cytokines such as CCL3, CCL2, CXCL1, TNF-α, and IL-6 during PVM infection.

In the context of respiratory viral infections, alveolar macrophages are key mediators of viral clearance and disease resolution *in vivo* (Tumpey et al., 2005; Kolli et al., 2014). One group recently showed that depletion of alveolar macrophages prior to RSV infection resulted in increased virus titers in the lungs, exacerbated disease and lung inflammation (Kolli et al., 2014). P-I-P treatment is associated with enhanced viral clearance, reduced immunopathology and higher alveolar macrophage numbers in the lungs during lethal PVM infection. It is likely that the latter event provided P-I-P-treated mice with an advantage, as alveolar macrophages are known to dampen excess inflammatory responses within the lung microenvironment (Pribul et al., 2008).

It has been suggested that neutrophils may play an important role in the regulation of local immunity (Gabelloni et al., 2013). One study showed that uncontrolled influx of neutrophils during an active influenza infection leads to severe lung inflammation (Tate

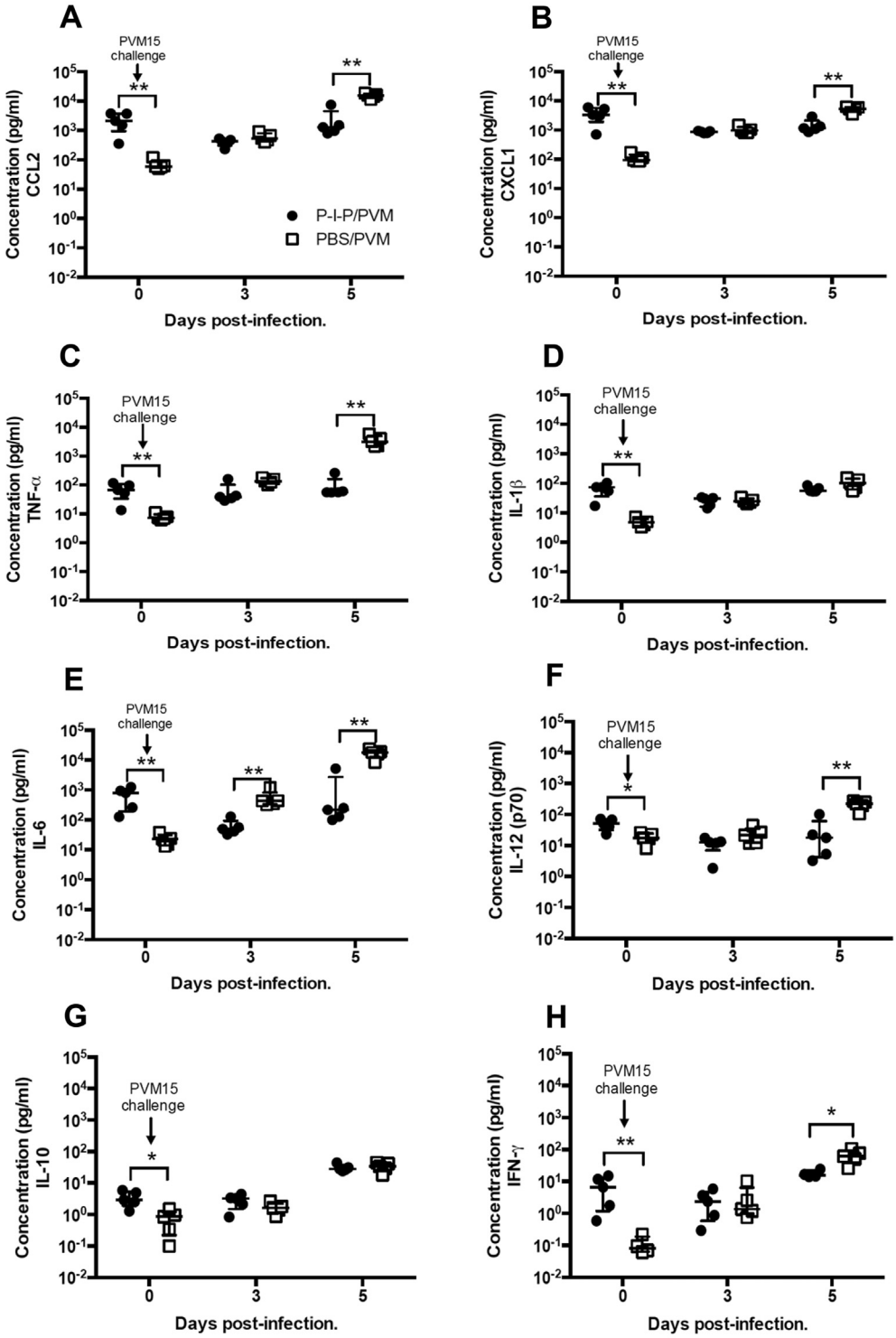

Fig. 8. Protein expression levels of chemokine and cytokine genes of P-I-P pre-treated PVM-infected Balb/c mice. Mice were given an intranasal treatment of PBS or P-I-P 24 h before challenge with 3000 pfu PVM. The multi-lobed lungs of 5 mice per group were collected separately for each individual animal on days 0 (prior to infection), 3 and 5 p.i. Protein expression was assayed by electrochemiluminescence-based multiplex ELISAs. Panels A to H represent protein expression data in pg/mL for CCL2, CXCL1, TNF-α, IL-1β, IL-6, total IL-12 (p70), IL-10, and IFN-γ, respectively. Data are shown as individual values representing single animals as well as median with interquartile range of five biological replicates. $^{*}p < 0.05$, $^{**}p < 0.01$.

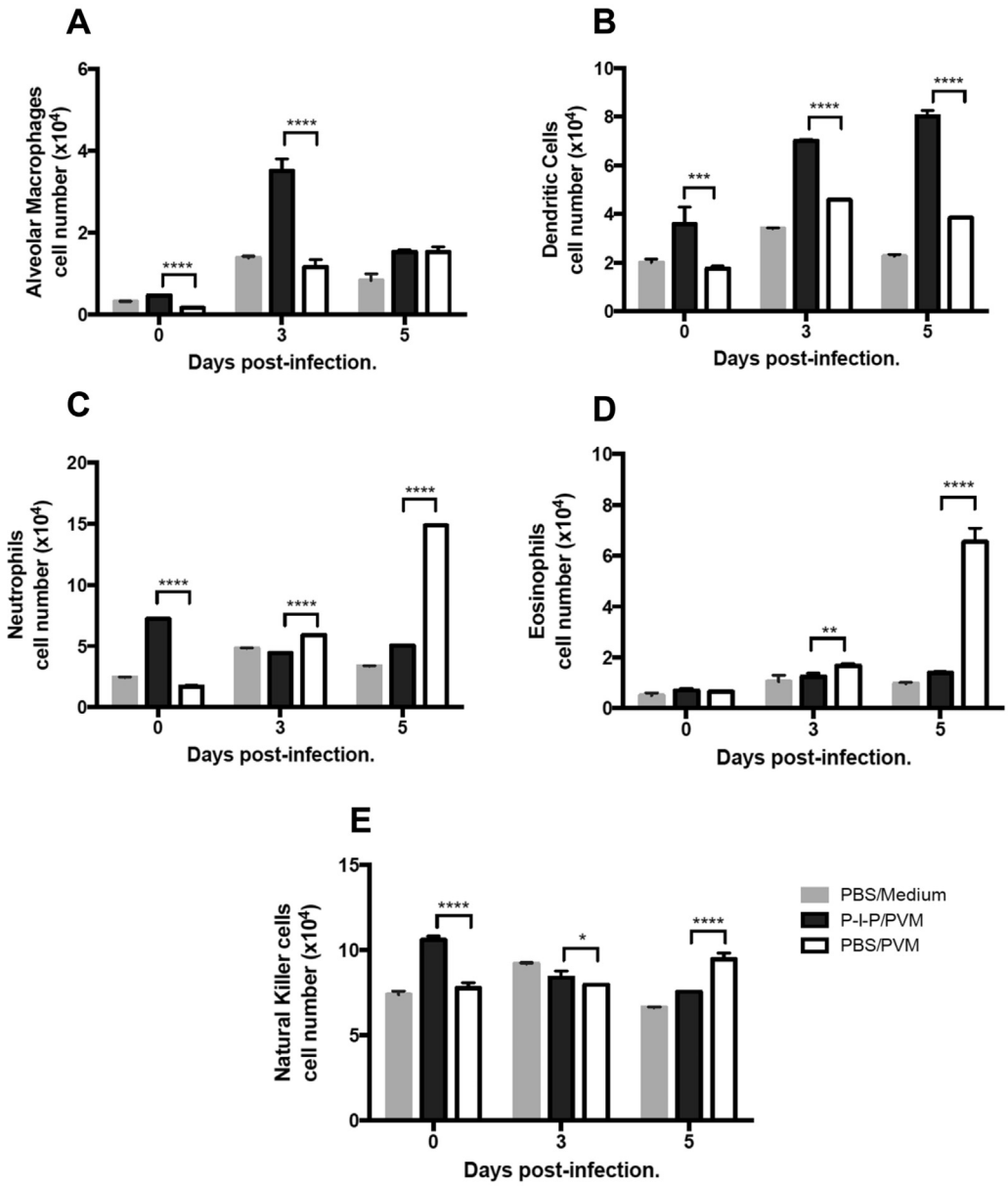

Fig. 9. Infiltration of immune cell populations into the lungs of P-I-P pre-treated Balb/c mice on days 0 (prior to infection), 3 and 5 following lethal PVM challenge. Mice were given an intranasal treatment of PBS or P-I-P 24 h prior to challenge with 3000 pfu PVM. The lungs of 3 mice per group were collected, pooled, and processed at the time points indicated. Following physical and chemical digestion of the tissue, single-cell suspensions were acquired. Total numbers of alveolar macrophages (A), DCs (B), neutrophils (C), eosinophils (D), and NK cells (E) in the lungs were analyzed by flow cytometry. Results are presented as cell number x 10^4 per million cells. Data are shown as the median with range of three technical replicates per cell type assayed. *$p < 0.05$, **$p < 0.01$, ***$p < 0.001$, ****$p < 0.0001$.

et al., 2008; Drescher and Bai, 2013). Similarly, prominent granulocyte accumulation in the lungs is a hallmark of PVM infection, which eventually progresses to pulmonary edema and respiratory distress (Bonville et al., 2009). In contrast, one group showed that mice depleted from neutrophils before the establishment of influenza A infection resulted in increased morbidity and mortality (Tumpey et al., 2005; Drescher and Bai, 2013). This evidence suggests that neutrophil infiltration, if properly controlled, can be beneficial by reducing disease (i.e. promoting viral clearance). Interestingly, early neutrophil influx was detected in P-I-P-treated mice. While it is possible that the treatment mediates moderate neutrophil recruitment into the lungs by the production of chemo-attractants like CXCL1 and CXCL2, these mice did not show signs of neutrophilia.

We and others showed that NK cell recruitment takes place at later time points during PVM infection (Watkiss et al., 2013; van Helden et al., 2012), which is correlated to an increase in lung virus titers, suggesting that the NK cell recruitment occurs too late to be beneficial. Treatment with P-I-P had a direct effect on NK cell infiltration. This formulation mediated the expression of NK cell chemo-attractants in the lung (i.e. CCL2, CCL3, CXCL10). Once within the tissue, these cells are likely to find an optimal environment that supports their activation and autocrine production of IFN-γ (Vivier et al., 2008). Consequently, IFN-γ can act directly on alveolar macrophages, leading to their activation and increased phagocytic activity (Schroder et al., 2004). The advantage of P-I-P is that these mice had an early local antiviral immune response prior to PVM exposure.

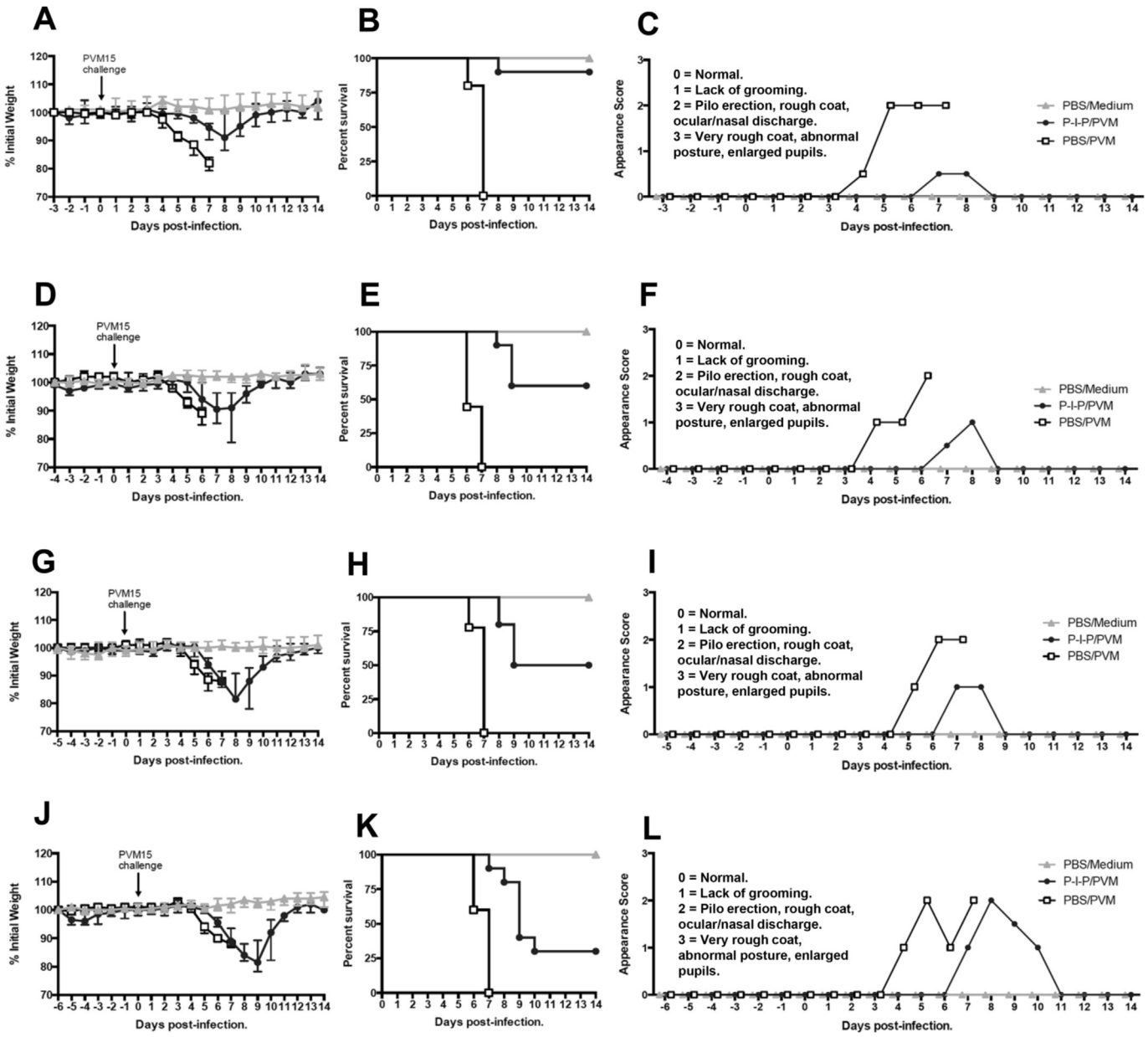

Fig. 10. Percent weight loss, survival and external appearance clinical scores of Balb/c mice treated with P-I-P or PBS 3 days (panels A–C), 4 days (panels D–F), 5 days (panels G–I) and 6 days (panels J–L) prior to intranasal PVM challenge. Mice were given prophylactic intranasal treatment of PBS or P-I-P at the time points indicated above, followed by a 3000 pfu PVM challenge. Animals were weighed and scored daily after treatment and for 14 days following infection. Data for weight loss is represented as the median percentage of the starting weight with error bars indicating the interquartile range. Percent survival rates are expressed as the median percentage of the total number of animals per group during the 14 days following infection. Clinical scores for external appearance are presented as the median value for each group during the entirety of the animal trial. Each experiment was performed twice, with an average of n = 5, and a total number of animals equal to 10 per group.

We propose that P-I-P can be used prophylactically for the prevention of RSV infections in high-risk populations like the elderly, who possess immune systems that do not perform optimally due to immune senescence. These individuals could be treated with the P-I-P formulation during outbreaks of RSV or possibly other respiratory infections such that partial immune protection can be provided. P-I-P acts primarily at level of the innate immune system of the host, which allows us to speculate on the possibility of a well-established P-I-P therapy to protect patients from multiple viral infections at once. It would be beneficial if one can protect the most vulnerable populations from major diseases like influenza, coronavirus, and RSV infections as most of these tend to be transmitted through the same route of exposure and during the same seasons. Studies confirming such pleiotropic effect are yet to be performed.

Acknowledgements

The authors would like to thank Laura Latimer, and Indranil Sarkar for technical assistance, as well as Sherry Tetland and Jan Erickson for the handling and care of the animals. This work was supported by grant number 119473 from the Canadian Institute of Health Research (CIHR). Elisa C. Martinez was supported by scholarships from the College of Graduate Studies and Research as well as the College of Medicine, University of Saskatchewan, Canada. This is VIDO-InterVac manuscript number 777.

Appendix A. Supplementary data

Supplementary data related to this article can be found at http://dx.doi.org/10.1016/j.antiviral.2016.10.008.

References

Awate, S., Wilson, H.L., Lai, K., Babiuk, L.A., Mutwiri, G., 2012. Activation of adjuvant core response genes by the novel adjuvant PCEP. Mol. Immunol. 51, 292–303.

Bem, R.A., Domachowske, J.B., Rosenberg, H.F., 2011. Animal models of human respiratory syncytial virus disease. Am. J. Physiol. Lung Cell Mol. Physiol. 301, L148–L156.

Bonville, C.A., Easton, A.J., Rosenberg, H.F., Domachowske, J.B., 2003. Altered pathogenesis of severe pneumovirus infection in response to combined antiviral and specific immunomodulatory agents. J. Virol. 77, 1237–1244.

Bonville, C.A., Percopo, C.M., Dyer, K.D., Gao, J., Prussin, C., Foster, B., Rosenberg, H.F., Domachowske, J.B., 2009. Interferon-gamma coordinates CCL3-mediated neutrophil recruitment in vivo. BMC Immunol. 10, 14.

Drescher, B., Bai, F., 2013. Neutrophil in viral infections, friend or foe? Virus Res. 171, 1–7.

Easton, A.J., Domachowske, J.B., Rosenberg, H.F., 2004. Animal pneumoviruses: molecular genetics and pathogenesis. Clin. Microbiol. Rev. 17, 390–412.

Gabelloni, M.L., Trevani, A.S., Sabatte, J., Geffner, J., 2013. Mechanisms regulating neutrophil survival and cell death. Semin. Immunopathol. 35, 423–437.

Garg, R., Shrivastava, P., van Drunen Littel-van den Hurk, S., 2012. The role of dendritic cells in innate and adaptive immunity to respiratory syncytial virus, and implications for vaccine development. Expert Rev. Vaccines 11, 1441–1457.

Garg, R., Latimer, L., Gerdts, V., Potter, A., van Drunen Littel-van den Hurk, S., 2014. Vaccination with the RSV fusion protein formulated with a combination adjuvant induces long-lasting protective immunity. J. Gen. Virol. 95, 1043–1054.

Garg, R., Latimer, L., Simko, E., Gerdts, V., Potter, A., van den Hurk, S., 2014. Induction of mucosal immunity and protection by intranasal immunization with a respiratory syncytial virus subunit vaccine formulation. J. Gen. Virol. 95, 301–306.

Garg, R., Latimer, L., Gerdts, V., Potter, A., van Drunen Littel-van den Hurk, S., 2015. The respiratory syncytial virus fusion protein formulated with a novel combination adjuvant induces balanced immune responses in lambs with maternal antibodies. Vaccine 33, 1338–1344.

Graham, B.S., Anderson, L.J., 2013. Challenges and opportunities for respiratory syncytial virus vaccines. Curr. Top. Microbiol. Immunol. 372, 391–404.

Hilchie, A.L., Wuerth, K., Hancock, R.E., 2013. Immune modulation by multifaceted cationic host defense (antimicrobial) peptides. Nat. Chem. Biol. 9, 761–768.

Hurwitz, J.L., 2011. Respiratory syncytial virus vaccine development. Expert Rev. Vaccines 10, 1415–1433.

Kolli, D., Gupta, M.R., Sbrana, E., Velayutham, T.S., Chao, H., Casola, A., Garofalo, R.P., 2014. Alveolar macrophages contribute to the pathogenesis of human metapneumovirus infection while protecting against respiratory syncytial virus infection. Am. J. Respir. Cell Mol. Biol. 51, 502–515.

Kovacs-Nolan, J., Latimer, L., Landi, A., Jenssen, H., Hancock, R.E., Babiuk, L.A., van Drunen Littel-van den Hurk, S., 2009. The novel adjuvant combination of CpG ODN, indolicidin and polyphosphazene induces potent antibody- and cell-mediated immune responses in mice. Vaccine 27, 2055–2064.

Morton, D.B., Griffiths, P.H., 1985. Guidelines on the recognition of pain, distress and discomfort in experimental animals and an hypothesis for assessment. Vet. Rec. 116, 431–436.

Mutwiri, G., Benjamin, P., Soita, H., Townsend, H., Yost, R., Roberts, B., Andrianov, A.K., Babiuk, L.A., 2007. Poly[di(sodium carboxylatoethylphenoxy) phosphazene] (PCEP) is a potent enhancer of mixed Th1/Th2 immune responses in mice immunized with influenza virus antigens. Vaccine 25, 1204–1213.

Nijnik, A., Madera, L., Ma, S., Waldbrook, M., Elliott, M.R., Easton, D.M., Mayer, M.L., Mullaly, S.C., Kindrachuk, J., Jenssen, H., Hancock, R.E., 2010. Synthetic cationic peptide IDR-1002 provides protection against bacterial infections through chemokine induction and enhanced leukocyte recruitment. J. Immunol. 184, 2539–2550.

Pribul, P.K., Harker, J., Wang, B., Wang, H., Tregoning, J.S., Schwarze, J., Openshaw, P.J., 2008. Alveolar macrophages are a major determinant of early responses to viral lung infection but do not influence subsequent disease development. J. Virol. 82, 4441–4448.

Rosenberg, H.F., Bonville, C.A., Easton, A.J., Domachowske, J.B., 2005. The pneumonia virus of mice infection model for severe respiratory syncytial virus infection: identifying novel targets for therapeutic intervention. Pharmacol. Ther. 105, 1–6.

Schroder, K., Hertzog, P.J., Ravasi, T., Hume, D.A., 2004. Interferon-gamma: an overview of signals, mechanisms and functions. J. Leukoc. Biol. 75, 163–189.

Shaw, C.A., Ciarlet, M., Cooper, B.W., Dionigi, L., Keith, P., O'Brien, K.B., Rafie-Kolpin, M., Dormitzer, P.R., 2013. The path to an RSV vaccine. Curr. Opin. Virol. 3, 332–342.

Shrivastava, P., Atanley, E., Sarkar, I., Watkiss, E., Gomis, S., van Drunen Littel-van den Hurk, S., 2015. Blunted inflammatory and mucosal IgA responses to pneumonia virus of mice in C57BL/6 neonates are correlated to reduced protective immunity upon re-infection as elderly mice. Virology 485, 233–243.

Tate, M.D., Brooks, A.G., Reading, P.C., 2008. The role of neutrophils in the upper and lower respiratory tract during influenza virus infection of mice. Respir. Res. 9, 57.

Tewari, K., Flynn, B.J., Boscardin, S.B., Kastenmueller, K., Salazar, A.M., Anderson, C.A., Soundarapandian, V., Ahumada, A., Keler, T., Hoffman, S.L., Nussenzweig, M.C., Steinman, R.M., Seder, R.A., 2010. Poly(I: C) is an effective adjuvant for antibody and multi-functional CD4+ T cell responses to Plasmodium falciparum circumsporozoite protein (CSP) and alphaDEC-CSP in non human primates. Vaccine 28, 7256–7266.

Tumpey, T.M., Garcia-Sastre, A., Taubenberger, J.K., Palese, P., Swayne, D.E., Pantin-Jackwood, M.J., Schultz-Cherry, S., Solorzano, A., Van Rooijen, N., Katz, J.M., Basler, C.F., 2005. Pathogenicity of influenza viruses with genes from the 1918 pandemic virus: functional roles of alveolar macrophages and neutrophils in limiting virus replication and mortality in mice. J. Virol. 79, 14933–14944.

van Helden, M.J., van Kooten, P.J., Bekker, C.P., Grone, A., Topham, D.J., Easton, A.J., Boog, C.J., Busch, D.H., Zaiss, D.M., Sijts, A.J., 2012. Pre-existing virus-specific CD8(+) T-cells provide protection against pneumovirus-induced disease in mice. Vaccine 30, 6382–6388.

Vivier, E., Tomasello, E., Baratin, M., Walzer, T., Ugolini, S., 2008. Functions of natural killer cells. Nat. Immunol. 9, 503–510.

Watkiss, E.R., Shrivastava, P., Arsic, N., Gomis, S., van Drunen Littel-van den Hurk, S., 2013. Innate and adaptive immune response to pneumonia virus of mice in a resistant and a susceptible mouse strain. Viruses 5, 295–320.

Wu, M., Hancock, R.E., 1999. Improved derivatives of bactenecin, a cyclic dodecameric antimicrobial cationic peptide. Antimicrob. Agents Chemother. 43, 1274–1276.

Zhao, J., Wohlford-Lenane, C., Zhao, J., Fleming, E., Lane, T.E., McCray Jr., P.B., Perlman, S., 2012. Intranasal treatment with poly(I*C) protects aged mice from lethal respiratory virus infections. J. Virol. 86, 11416–11424.